AD-A104 216 GEORGIA INST OF TECH ATLANTA CENTER FOR THE ADVANCEM--ETC F/G 11/6
AN ANALYSIS OF, AND SOME OBSERVATIONS ON, DYNAMIC FRACTURE IN A--ETC(U)
JUL 81 T NISHIOKA, M PERL, S N ATLURI N00014-78-C-0636
UNCLASSIFIED GIT-CACM-SNA-10 NL

1 OF 1
AD A
104216

END
DATE FILMED
10-81
DTIC

LEVEL

Office of Naval Research

Contract N00014-78-C-0636 NR 064-610

Technical Report No. 12

Report No. GIT-CACM-SNA 10

AN ANALYSIS OF, AND SOME OBSERVATIONS ON, DYNAMIC FRACTURE IN AN IMPACT TEST SPECIMEN

by

T. Nishioka, M. Perl, S.N. Atluri

July 1981

Center for the Advancement of Computational Mechanics
School of Civil Engineering
Georgia Institute of Technology
Atlanta, Georgia 30332

81-PVP-10

THE AMERICAN SOCIETY OF MECHANICAL ENGINEERS
345 E 47 St., New York, N.Y. 10017

An Analysis of, and Some Observations on, Dynamic Fracture in an Impact Test Specimen

T. Nishioka
Research Scientist II

M. Perl
Research Scientist II

S. N. Atluri
Regents' Professor of Mechanics

Center for the Advancement of Computational Mechanics
School of Civil Engineering,
Georgia Institute of Technology,
Atlanta, Ga. 30332

Numerical simulations of crack-propagation histories in four cases of dynamic tear test experiments on 4340 steel are performed. The influence of the loss of contact of the specimen at various times with either the supports or the tup or both is critically examined. In each case, the variation of the dynamic K-factor, for the simulated crack-propagation history, is directly computed. The results are discussed in the light of current controversies surrounding the dynamic fracture toughness properties governing crack-propagation under impact loading. It is concluded that these controversies may not be fully warranted.

ABSTRACT

Numerical simulations of crack-propagation histories in four cases of dynamic tear test experiments on 4340 steel are performed. The influence of the loss of contact of the specimen at various times with either the supports or the tup or both is critically examined. In each case, the variation of the dynamic K-factor, for the simulated crack-propagation history, is directly computed. The results are discussed in the light of current controversies surrounding the dynamic fracture toughness properties governing crack-propagation under impact loading. It is concluded that these controversies may not be fully warranted.

INTRODUCTION

Until recently, for stituations governed by small-scale yielding, it was thought that the governing criterion for elastodynamic crack propagation under Mode I plane strain conditions can be written as: $K_I(v,t) = K_{ID}(v)$, where $K_{ID}(v)$ is the velocity-dependent fracture toughness of the material, which was thought to be a "reasonable" geometry-independent material property. This hypothesis appeared to have been validated in several studies related to dynamic crack-propagation initiated under quasi-static loading. In the analysis of such cases, both "generation" and "propagation" calculations were employed: in the former calculation, the experimentally measured crack-propagation history was simulated to find the stress-intensity factor or the velocity-dependent fracture toughness: the latter calculation was used in either of the two-ways (i) based on a given K_{ID} versus v relation to find the crack propagation history, or (ii) to find the best K_{ID} versus v relation, the calculated crack-propagation history corresponding to which, agreed best with the experiment. The remarkable success of these calculations appeared to indicate that the prediction of dynamic crack-propagation and possible arrest under general loading conditions may be well within the grasp of current art of computational mechanics.

Recently some work has appeared, however, that seemed to cast doubt on the concept of dynamic fracture toughness that is independent of the rate of applied loading. In Ref.[1], Kanninen et al reported experimental and numerical results on dyanamic tear test specimens of 4340 steel, a high-strength, rate-insensitive material. In these experiments, crack-propagation was initiated from notches, of varying degree of "bluntness", under impact as well as quasi-static loading. The dynamic fracture-toughness was attempted to be inferred from the energy measured to be absorbed in the tear test. A series of "propagation type" linear elasto-dynamic analyses, using hypothetical K_{ID} values, were performed. A surprising finding of [1] was that the dynamic fracture toughness governing crack-propagation initiated from a blunted crack-tip under impact loading may be significantly higher (roughly 170) than when crack-growth is initiated quasi-statically (roughly about $65 MNm^{-1.5}$).

The primary objective of the present paper is an attempt to analyze the data presented in [1] and to examine the results in the light of the conclusions presented in [1]. In addition to the blunt-notch specimen data reported in [1], analysis is performed also of the data for a fatigue pre-cracked specimen supplied to the authors by the Battelle Columbus Laboratories in January 1981. In the present paper, in contrast to those in [1], "generation" type calculations are employed, i.e., the experimental data for crack-velocity versus time history is simulated in a finite element program to determine

Contributed by the Pressure Vessels & Piping Division of The American Society of Mechanical Engineers for presentation at the Joint Conference of the Pressure Vessels and Piping, Materials, Nuclear Engineering and Solar Divisions, June 21-25, 1981, Denver, Colorado. Manuscript received at ASME Headquarters March 25, 1981.

Copies will be available until March 1, 1982.

directly the stress-intensity factor variation with time. The employed finite element method is the "moving-singularity" procedure reported earlier by the authors [2, 3]. In the present analysis, careful attention is paid to the boundary conditions on the specimen, especially the loss of contact of the specimen at various times with either the supports, or the tup, or both. Four different cases of experimental specimen are analyzed. In each case, the input energy, kinetic energy, elastic energy, and fracture energy variations are computed. It is noted that each of these energy quantities is computed directly in the present procedure. That these energy quantities "blance out" is nothing but an a posteriori check on the present calculations. It should thus be noted that, in contrast to the "propagation" calculations in [1], fracture energy is not inferred from an energy balance, but directly computed in the present "generation" calculation.

Detailed results are presented for each of the four cases analyzed. These results are analyzed to arrive at some "plausible" conclusions which appear to be at variance with the conclusions presented in [1].

ANALYSIS

The test specimen geometry is indicated in Fig. 1, along with the finite element mesh employed in the modeled portion of the specimen. Points L and S in Fig. 1 represent, respectively, the loading and support points. Sixty-two 8-noded isoparametric elements and one moving singularity element are used. The specimen geometry indicated in Fig. 1 corresponds to that reported in [1], and a plane-strain condition is invoked in the present two-dimensional analysis. In simulating the experiments [1], the following initial conditions are used in the present analysis: at time t=0, velocity $\dot{\bar{u}}_L$=6.88m/sec. The tup displacements are calculated by $\bar{u}_L=\dot{\bar{u}}_L t$. The present analysis does not account for the elasticity of either the tup or the supports, largely due to the lack of knowledge to quantify such.

In all but one of the present four series of calculations, account is taken of the possibility of lack of contact of the specimen with either the tup or the supports (i.e., the tup and supports can "push" the specimen but not "pull") at various instants of time, as and when the analysis may naturally dictate. In one case, to study the effect of the above contact/no-contact conditions, the specimen was held "fixed" (i.e., the tup and supports are always in contact with the specimen).

Also, it is to be understood that the present series of computations are the so-called "simulation" or "generation" studies in the sense defined in [1], as opposed to the "propagation" studies performed in [1]. To the uninitiated, these terms imply: "generation study" means solving for the dynamic stress-intensity factor for a crack which is "made" to propagate with the experimentally measured crack-length (or crack-velocity) versus time history, while "propagation study" implies soving for the crack-length (or velocity) versus time history using a "hypothesized" dynamic fracture toughness (which may or may not depend on crack-velocity [1]) value.

The present series of computations are summarized in Table I.

Table I: "Generation Studies"

Study No \ Data	Notch-root Diameter	Initiation Time	Boundary Conditions
DTT 1	0.064mm	95 μsec.	Fixed
DTT 2	0.064mm	95 μsec.	Contact/ No-contact
DTT 3	0.064mm	35 μsec.	Contact/ No-contact
DTT 4	0.000mm	92.24 μsec.	Contact/ No-contact

The crack-length versus time histories for the above four cases are shown in Fig. 2. For the cases DTT 1 and DTT 2, the Δa vs t curves used are the same as that in Fig. 4 of Ref. [1], except that the boundary conditions are different as in Table 1. In Fig. 4 of Ref. [1], one date point indicating a crack-growth of ~ 2.5mm at t~45 μsec. is included, but this point was omitted in [1] in plotting the Δa vs t curve. In the present study designated as DTT 3 above, this data point was included in the Δa vs t curve, and further, the time of initiation of propagation was chosen such that the K value at initiation ~ 65MNm$^{-1.5}$; this curve is shown in Fig. 2. DTT 4 indicates the data obtained from M.F. Kanninen [4] for a fatigue pre-cracked specimen; however, the initiation time was determined to be 92.24 sec. by extrapolation of the supplied [4] experimental data.

Prior to the presentation of the results, we indicate briefly the analysis procedure. As noted earlier, the present analysis of dynamic crack propatation is based on the procedure developed by the authors, and detailed elsewhere [2, 3]. To supplement the mathematical procedures in [2, 3] for the present case, we consider some details of imposing "contact/no-contact" boundary conditions on the specimen.

We designate the force with which either the tup or the supports "push" the specimen as being (+ ve). Using the standard notation, the reaction forces at the points where displacements are prescribed are calculated by:

$$\underset{\sim}{P} = \underset{s}{K}\underset{\sim}{q} + \underset{s}{m}\ddot{\underset{\sim}{q}}. \qquad (1)$$

The displacement u and reaction force P in the time step (n+1) are predicted by:

$$u_{n+1} = u_n + \Delta t_{n+1}\dot{u}_n \qquad (2)$$

and

$$P_{n+1} = P_n + \frac{(P_n - P_{n-1})}{\Delta t_n}\Delta t_{n+1}. \qquad (3)$$

It is noted that we may use $\Delta t_{n+1}=\Delta t_n=\Delta t$. Assume that P_{n-1} and P_n are (+ ve) and that $P_{n-1}>P_n$. The no-contact condition during the time increment (n) to (n+1) is predicted to occur after the sub-increment of time:

$$\Delta t_C = \frac{P_n}{(P_{n-1}-P_n)}\,\Delta t. \qquad (4)$$

If $0 \le \Delta t_C \le \Delta t$, during the (n+1) step, we change Δt to Δt_C and perform the analysis with condition of contact and during (n+2) step, we change Δt to Δt_F ($\Delta t_C + \Delta t_F = \Delta t$), and perform the analysis with the condition of no-contact. This process is repeated.

An analogous scheme is used to predict the transition from a "no-contact" to "contact" condition; however, this time by monitoring the displacements of the respective points of the specimen relative to either the supports or the tup.

RESULTS

First we consider the DTT 1 case. In this case, the displacement, velocity, and acceleration at the point L (see Fig. 1) are prescribed. L_1, L_2 and L_3 as shown in Fig. 3 are the times when the reaction force at the tup becomes zero (note "+ ve reaction" implies that the tup is pushing the specimen). Negative "reaction force" is observed during times $L_1<t<L_2$, and $t>L_3$. This phenomenon can also be observed in the experiments of Mall et al [5]. Since the tup contact time measured in the experiment [1] was about 180 μsec., the computation was stopped at around this time. Fig. 4 shows the variation of the computed stress intensity factors in the present "generation" or "simulation" study. The times marked by 'v_1' and 'v_2' in Fig. 4 are the times when the crack propagates with constant velocities v_1 and v_2 respectively (see [1]). The initiation toughness K_{Id} (the terminology is summarized later in this paper) obtained in this computation, as seen from Fig. 4 is about $106 MNm^{-1.5}$. The computed variation of input, strain, kinetic, and fracture energies with time, are shown in Fig. 5. It is noted that in the present procedure [2, 3] the dynamic K-factors are solved for, directly. From this, the energy release-rate is calculated. Alternatively, fracture energy is also calculated directly from a crack-tip integral of work done in separation of crack-faces. These two procedures, discussed in [6], were noted to give almost identical results for the present cases). It is noted that each of the four energies, input, strain, kinetic, and fracture, are calculated independently, in the DTT 1 case as well as the other three cases, in the present work. That these energies "balance" is an independent, a posteriori check on the present calculations. It is seen from Fig. 5 that during the periods $L_1<t<L_2$ and $t>L_3$ input energy appears to actually decrease, due to "negative reaction forces" during these times as discussed earlier. We will comment further on those energy variations later. Fig. 6 shows the crack opening profiles at various times. As seen, the profiles are nearly linear except very near the crack-tip. This suggests the possibility of developing K_I measurement techniques from crack-opening displacements, in dynamic tear testing. Fig. 7 shows the contours of equivalent stress σ_e in the presently used singular element, which is shown hatched in Fig. 1. As seen, the stress level reaches that of yield, σ_{ys}, only within the contour shown by a broken line in Fig. 7. The maximum distance of this cotour is roughly 0.5mm from the crack-tip; thus indicating the insignificant role of plasticity in the present problem. Contours of principal-stress difference (which may be used in a Tresca-type yield condition) shown in Fig. 8, can be observed to be more or less similar to those of equivalent stress (which may be used in a Mises-type yield condition) shown in Fig. 7.

We now consider the case labeled DTT 2 in Table 1. It is noted that the condition of contact/no-contact was invoked in this case. As seen from Fig. 9, the specimen is not in contact with the tup during the periods $L_1<t<L_2$; $L_3<t<L_4$, and $t>L_5$ as marked. Also, it can be seen from Fig. 10 that the specimen is not in contact with the supports during the times $S_1<t<S_2$, and $t>S_3$ as marked in Fig. 10. Comparing Figs. 9 and 10 it is seen that the maximum reaction force P_s, at the support point, is very close to the maximum tup load, P_L. The variation of the computed dynamic K-factor is shown in Fig. 11. It is seen that the initiation toughness, K_{Id} is again about $108 MNm^{-1.5}$. However, prior to initiation, K_I value appears to reach $122 MNm^{-1.5}$ ($>K_{Id}$) at t=82 μsec. Comparing Figs. 9 and 10, it is seen that during the times $L_1<t<S_2$, $S_3<t<L_4$, and $t>L_5$, the specimen is not in contact with either the tup or the support, i.e., the specimen is a free-flying object! Fig. 12 shows the variation of the four energy quantitites; input, kinetic, elastic, and fracture. During $L_1<t<L_2$, $L_3<t<L_4$ and $t>L_5$, since the specimen looses contact with the tup, no increase in input energy occurs, as seen from Fig. 12. It is noted from Fig. 12 that the total work done at ≈180 μsec. was about 53 Joules. This is less than half of the experimentally measured absorbed-energy value of 130 Joules. However, in the present analysis, no account is taken of energy dissipated, if any, in the supports or the tup. This discrepancy, while of no consequence in the present "generation-type" study (wherein energy-balance calculations are "by-products" of the analysis), can have deleterious consequences on a "propatation"-type study as in [1] wherein the experimentally measured absorbed-energy is used in inferring the fracture energy, from which a "plausible" fracture-toughness value is calculated [1]. This is an important point to remember in comparing the present results and those in [1]. In Fig. 13, the crack-opening displacements in cases DTT 1 and DTT 2 are compared. It is seen that the COD in DTT 2 oscillates around the values in DTT 1 case.

Now, we consider the DTT 3 case. The tup contact-force variation is shown in Fig. 14. Comparing Figs. 9 and 14, it is seen that during $L_1<t<L_2$, the separation between the specimen and the tup, $(u_L-\bar{u}_L)$ is bigger than in the DTT 2 case. This is attributed to the higher compliance of the DTT 3 specimen due to the fact that growth initiation occurs much earlier. Also the second loss of contact of the specimen and the tup ($L_3<t<L_4$) and the second peak of P_L ($L_2<t<L_3$) are smaller than those in the case of the DTT 2 specimen. Fig. 15 shows the displacement of the specimen from the support point, and the support reaction force. Comparing Figs. 10 and 15 it is seen that the periods S_1-S_2 and S_2-S_3 are longer than those of the DTT 2 specimen; and the peak value of P_s is smaller than that of DTT 2. Again,

these tendencies can be attributed to the earlier crack initiation in this specimen. Fig. 16 shows the K-factor variation. Note that, as shown in Table I, the crack growth initiation time was chosen to be t=35 μsec. such that K_{Id}=65MNm$^{-1.5}$. In spite of this, the K-factor variation in DTT 3 is more or less identical to that in DTT 2 (Fig. 11) until about t=95μsec. During the period of t=95 μsec. to 146 μsec., the K value in DTT 3 decreases while that of DTT 2 increases. The variation of total work, strain energy, and fracture energy are shown in Fig. 17. It is seen that during $v_1<t<v_3$, a very small amount of energy is consumed in the fracture process.

Finally, we consider the DTT 4 case. The tup contact-force variation is shown in Fig. 18. As seen from Fig. 2, the crack propagates faster in DTT 4 case than in the DTT 2 case. Due to this reason, the changed compliances, the second peak of P_L ($L_2<t<L_3$) is smaller, and the second separation between the specimen and the tup, i.e., $(u_L-\bar{u}_L)$ between$(L_3<t<L_4)$, is larger in the DTT 4 case than in DTT 2. The support reactions, and separation between supports and specimen, are shown in Fig. 19. These are more or less similar to those in the DTT 2 specimen. From the K-factor variation shown in Fig. 20, it is seen that the K_{Id} value is about 111MNm$^{-1.5}$. After initiation, K drops significantly. The energy variation plots are given in Fig. 21, from which it is seen that the total energy to the specimen is lower than in the other three cases.

In the following we attempt to draw some rational conclusions from the above presented numerical data.

Comments on Fracture in Impact Specimens

At the outset, we define the following nomenclature:

K_{IC}: Plane-strain fracture toughness under quasi-static loading

K_{ID}: (Variable) Dynamic fracture toughness for a propagating crack

K_{Id}: Initiation fracture toughness under dynamic loading

K_Q: "Apparent" fracture toughness at initiation with a blunt notch under quasi-static loading

K_{Qd}: "Apparent" fracture toughness at initiation with a blunt notch under dynamic loading

$K_{ID,min}$: Lower bound, if any, for K_{ID}.

A typical K_{ID} versus crack-velocity curve widely reported in literature is given in Fig. 22. For most brittle materials, $K_{ID,min}$ appears to be lower than K_{IC}, and:

$$K_{ID,min} = 0.5 \text{ to } 1.0\ K_{IC}. \qquad (5)$$

The governing equation for elastodynamic crack propagation, currently considered to be valid under quasi-static loading conditions, can be expressed by:

$$K_I(t,v) = K_{ID}(v) \qquad (6)$$

where K_{ID} is a function of crack-velocity. In general, the above equation is inconsistent, from a functional view-point, at the point of crack-growth initiation. For example, if the "crack" starts propagating (i.e., attains a finite velocity in zero-time) from a blunt notch with an intensity value K_Q, we have:

$$K_I = K_Q(b) \neq K_{ID,min}$$

where b is the notch-root diameter. Moreover, for initiation under quasi-static loading from a sharp notch or a fatigue crack [b=0], wherein the crack is assumed to attain a finite velocity in zero time, we have:

$$K_I = K_{IC} \neq K_{ID,min} \qquad (8)$$

except in the special when $K_{ID,min}=K_{IC}$.

Now, under conditions of impact loading, the initiation fracture toughness K_{Id}, as reported in most of the literature, is generally lower than K_{IC}. The values of K_{Id}/K_{IC} as reported in literature are summarized in Table 2.

Table 2: Initiation Toughness Under Dynamic Loading

Investigators	Material	Temp °C	Load Rate $\dot{K}_I$[MNm$^{-1.5}$/sec.]	K_{Id}/K_{IC}
Shabbits [7]	A533B	10	10^4	-0.67
Kalthoff et al [8]	Araldite B	Ambient	10^4	-0.73
Mall et al [5]	Poly-carbonate	Ambient	6×10^3	-0.65
Ireland [9]	A533	10	10^6	-0.63
Ireland [9]	4340 Steel	20	Pre-cracked Charpy	-1.00

Influence of the rate of loading on K_{Id} is shown in Fig. 23, which is taken from Refs. [7, 9]. As seen from Fig. 23, for most of the materials, K_{Id} decreases with increasing $\dot{K}_I$. Fig. 24, taken from Ref. [10] shows the comparison of K_d, K_D (subscript I omitted due to the fact that plane-strain conditions were not validly met), and K_{IC} data for A533B steel. From table 2 and Figs. 23 and 24, one may observe that:

$$K_{Id} = K_{Id}(\dot{K}_I) = 0.5 \sim 1.0\ K_{IC}. \qquad (9)$$

Once again, Eq. (6) is functionally inconsistent at growth-initiation associated with an impact loading. Furthre, for growth-initiaion from a blunt notch under impact loading, we have:

$$K_I = K_{Qd}(b) (K_{Qd}>K_{Id} \text{ and } K_{Qd} \neq K_{ID,min}) \qquad (10)$$

However, after a certain amount of crack propagation,

... 6) may be applicable, in a rate-insensitive material, even under impact loading, although Eq. (6) is expressed for quasi-static loading. Contrary to this, for a rate-sensitive material under impact loading, the governing equation for dynamic crack propagation may differ from Eq. (6), and may be rewritten, possibly, as

$$K_I(t,v) = K_{ID}(v,\dot{\varepsilon}) \text{ or } K_{ID}(v,\dot{K}) \qquad (11)$$

where $\dot{\varepsilon}$ is the strain-rate in the vicinity of the crack-tip (see Fig. 25). If $\dot{\varepsilon}$ (or $\dot{K}$) is small, or the material is almost rate-insensitive, the situations in Fig. 25 a and b become practically the same.

It should be noted that all the analyses in Ref. [1] are of the "propagation" type in the sense defined earlier. In [1], the K_{ID} versus v curve for 4340 steel is first assumed as:

$$K_{ID} = 65 + 0.044\ v \qquad (12)$$

where K_{ID} is in $MNm^{-1.5}$ and v is in m/sec. In [1], the range of crack-velocity for which Eq. (12) is valid is not indicated. However, in general, there should be an upper-limit value for velocity as shown in Fig. 22. Additional evidence of an upper limiting value for velocity is shown in Fig. 26, taken from Ref. [10]. From Eq. (12), $K_{ID,min} = 65MNm^{-1.5}$ while K_{IC} appears to be about 50 from the Damage Tolerant Design Handbook [11], and Fig. 26. Considering the near rate-insensitive behavior of 4340 steel, it then appears that $K_{Id} \simeq K_{IC} \simeq K_{ID,min} \simeq 50\text{-}65MNm^{-1.5}$.

In order to sustain a running crack, the surrounding elastic field must produce plastic strains continually near the advancing crack-tip adequate for the separational process (region R of Fig. 25). If K_{Id} is considerably lower than $K_{ID,min}$ and the elastic field near the crack-tip cannot continually supply energy to the process zone, the crack will be arrested. In the above case if, on the other hand, the elastic field can continually supply energy to the process zone, the crack will propagate with a somewhat low velocity in the earlier stages of crack-propagation. This appears to be verified in the present set of simulations. Comparing the K_I variations in DTT 2 and DTT 3 specimens (Figs. 11 and 16 respectively) it is seen that the K_I variations are essentially similar eventhough the crack in the DTT 3 case has been assumed to propagate with an initiation value of $K_I = 65MNm^{-1.5}$. This can be attributed to the nature of the presently considered experiment in which the elastic field near the crack is always growing in intensity during the period t=10 to 80 μsec.

However, in the DTT 4 specimen, the present simulation indicates initiation thoughness of $\sim 110MNm^{-1.5}$ (see Fig. 20). However, as mentioned earlier, the initiation time for the DTT 4 case which was unknown in the experiment, was determined by extrapolation of the crack-growth versus time data. Thus, as can be rationalized from a comparison of the DTT 2 and DTT 3 cases, one may surmise that crack-growth initiation may have occured much before t=92 μsec. (as used in the present calculations, see Fig. 20), even if with a very small velocity. Therefore, one may postulate that even for the DTT 4 case, K_{Id} value may actually have been less than or equal to $65MNm^{-1.5}$. This hypothesis may in fact be considered to be also supported by the results of [1]. Reffering to Fig. 8 of [1], it is seen that in the "propagation" calculation, the use of the relation $K_{ID}=65+0.044v$ actually gives a much better agreement with the experiment in terms of crack-initiation time rather than the use of $K_{ID}=170MNm^{-1.5}$. Note that the experimental data for the first measurement of crack grwoth is missing in Fig. 8 in Ref. [1]. Contrary to this, after a certain amount of crack-growth, use of $K_{ID}=170MNm^{-1.5}$ appears to give a good agreement of the "propagation" calculation [1] with the experimental data.

However, as noted earlier, the value of $K_{ID}=170MNm^{-1.5}$ was "derived" in [1] from an energy balance consideration: the total energy absorbed during the impact fracture of specimen was 130 Joules; the energy imparted to an "intact" unconstrained specimen from an elastic collision between the top and specimen was 79 Joules; and the difference (130-79)=51 Joules was assumed to be consumed as fracture energy. From this assumed fracture energy and average fracture toughness value of $170MNm^{-1.5}$ was derived in [1]. Thus, the propagation analysis [1] represents an a priori "energy-balance" condition, in which other sources of energy dissipation are ignored. On the other hand, as already noted, in the present "generation" calculations, an energy balance relation is an a posteriori "by-product" of the calculation itself in which the experimental crack-growth history is simulated. In connection with Fig. 12, (DTT 2 specimen, which is also the basis for the computation $K_{ID}=170$ in Ref. [1]) it is noted that the computed total input to the specimen is 53 Joules, which is less than half of the experimentally measured value of 130 Joules! This brings to question the neglection of other dissipated energies, and hence the value of $K_{ID}=170MNm^{-1.5}$ hypothesized in [1].

The present analysis, and the above discussion, appear to lead us to believe that the use of K_{ID} versus v curve with $K_{ID,min} = 65MNm^{-1.5}$ and $K_{Id} \simeq 65MNm^{-1.5}$, with the curve being such that the upper value of v is limited (as in Fig. 22), may be warranted. Suppose this "saturated" curve is used in the "propagation" calculation; then the crack will start to propagate at t = 25 ≈ 35 μsec. During most of the period from initiation to about t = 100 μsec., the crack will propagate with a relatively slow velocity, as discussed earlier (i.e., crack growth will be small until about t ~ 100 μsec.). The crack will attain a higher velocity because of the nature of the testing system considered, in that K_I is increased continually by the dropping tup. Then the crack speed will saturate. In addition to the property of the "saturated" K_{ID} vs v curve, there may be other factors to limit the crack speed in the present type of specimen. One of these is the presence of the compressive stress field in the ligament of the specimen, as can be seen from the momentum balance condition.

Contrary to the impact loading, under quasi-static loading the analysis using $K_{ID}=65 + 0.044\ v$ gave good agreement with the experiment in [1]. In this case, since the tup was fixed to correspond to

K_Q=108MNm$^{-1.5}$, the value of K_I during crack-propagation under quasi-static loading condition is always lower than 108MNm$^{-1.5}$ [$K_I(t,v)<K_Q$]. This suggests that K_{ID}=65 + 0.044 v is valid for lower values of velocity, while this linear relation may be invalid for larger velocities, and eventually the velocity will be limited, leading to a satuarated K_{ID} versus v curve.

ACKNOWLEDGEMENTS

This work was supported by the Office of Naval Research under Contract Number N00014-78-C-0636. The authors gratefully acknowledge this support. The encouragement of Dr. Nicholas Perrone is thankfully acknowledged. The authors express their appreciation to Ms. Margarete Eiteman for her care in typing this manuscript.

REFERENCES

1 Kanninen, M.F., Gehlen, P.C., Barnes, C.R., Hoagland, R.G. and Hahn, G.T., "Dynamic Crack Propagation Under Impact Loading", in Nonlinear & Dynamic Fracture Mechanics, ASME Publication AMD-Vol 35, (N. Perrone & S.N. Atluri, Eds), pp 185-200, (1979).

2 Nishioka, T. and Atluri, S.N., "Numerical Modeling of Dynamic Crack Propagation in Finite Bodies, by Moving Singular Elements, Part I - Formulation", Journal of Applied Mechanics, Vol. 47, No. 3, pp 570-577, (1980).

3 Nishioka, T. and Atluri, S.N., "Numerical Modeling of Dynamic Crack Propagation in Finite Bodies, by Moving Singular Elements - Part II. Numerical Results", Journal of Applied Mechanics, Vol. 47, No. 3, pp 577-583, (1980).

4 Kanninen, M.F., Private Communication, Battelle's Columbus Labs, Jan. 1981.

5 Mall, S., Kobayashi, A.S. and Urabe, Y., "Dynamic Photoelastic and Dynamic Finite Element Analysis of Polycarbonate Dynamic Tear Test Specimens", Fracture Mechanics, ASTM STP 677 (C.W. Smith, Ed.) pp 498-510, (1979).

6 Nishioka, T., Stonesifer, R.B. and Atluri, S.N., "An Evaluation of Several Moving Singularity Finite Element Procedures for Analysis of Fast Fracture", Jnl. of Engineering Fracture Mechanics, (to appear), 1981.

7 Shabbits, W.O., "Dynamic Fracture Toughness Properties of Heavy Section A533B Class 1 Steel Plate" WCAP-7623, HSST Program Technical Report, (1970).

8 Kalthoff, J.F., Winkler, S. and Beinert, J., "The Influence of Dynamic Effects in Impact Testing", Intl. Jnl. of Fracture, Vol. 13, pp 528-531, (1977)

9 Ireland, D.R., "Critical Review of Instrumental Impact Testing", Dynamic Fracture Toughness, Proc. of an Int. Conf. arranged by the Welding Institute, and the Am. Soc. Metals, July 5-7, 1976, London, pp 47-62.

10 Hahn, G.T., Hoagland, R.G. and Rosenfield, A.R., "Fast Fracture Toughness of Steels", Dynamic Fracture Toughness, pp 237-247, (1976).

11 Damage Tolerance Deisgn Handbook, Metals and Ceramics Informatin Center, Battelle Columbus Labs, 1975.

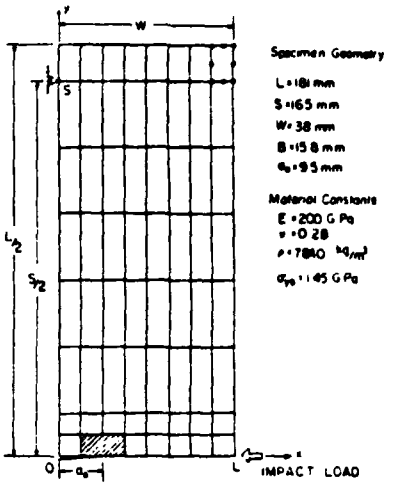

Figure 1

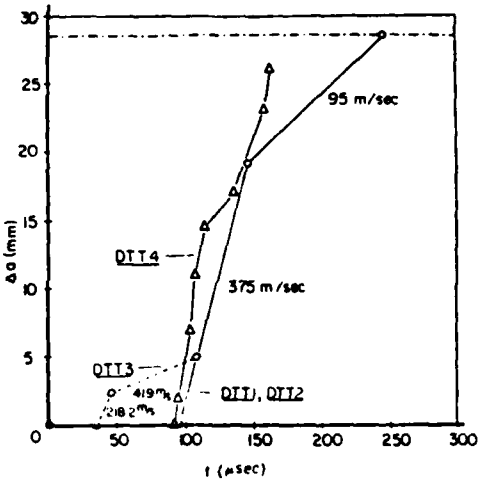

Figure 2

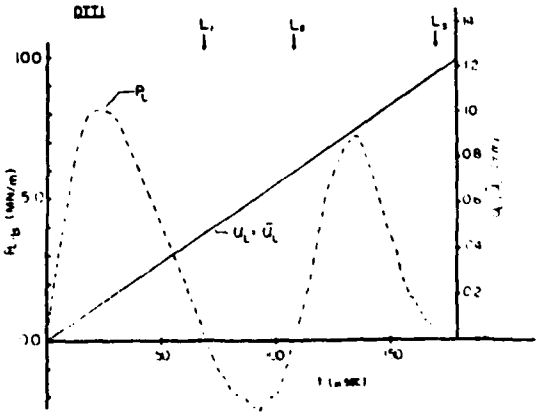

Figure 3

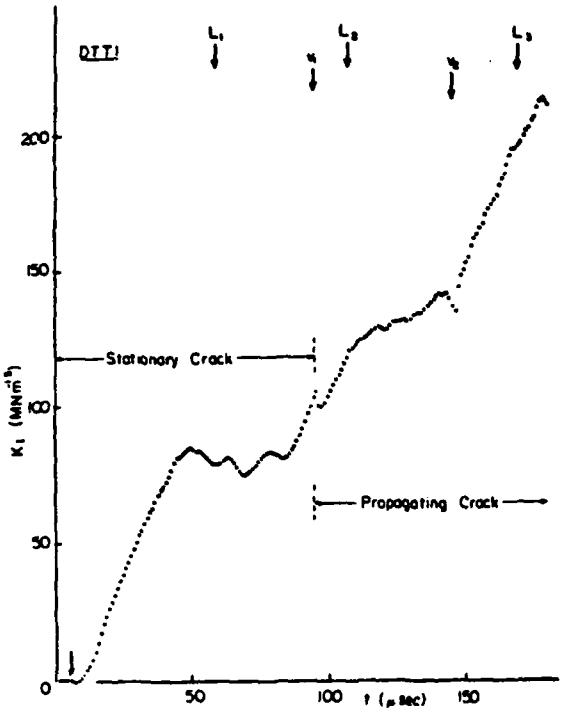

Figure 4

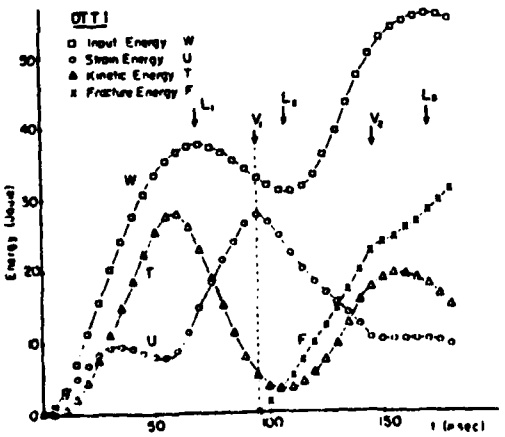

Figure 5

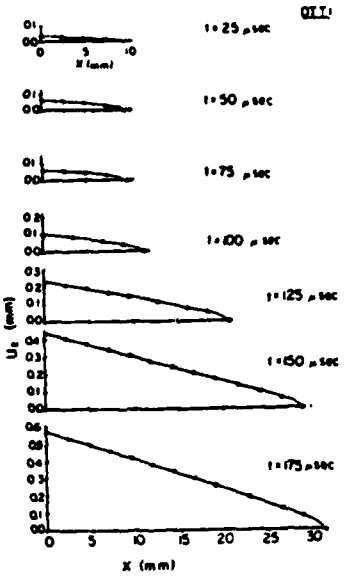

Figure 6

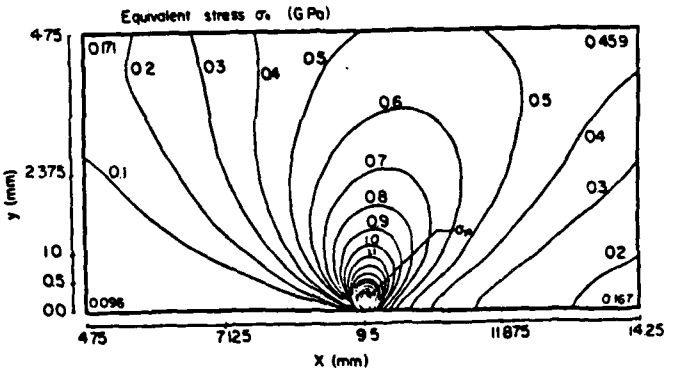

Figure 7

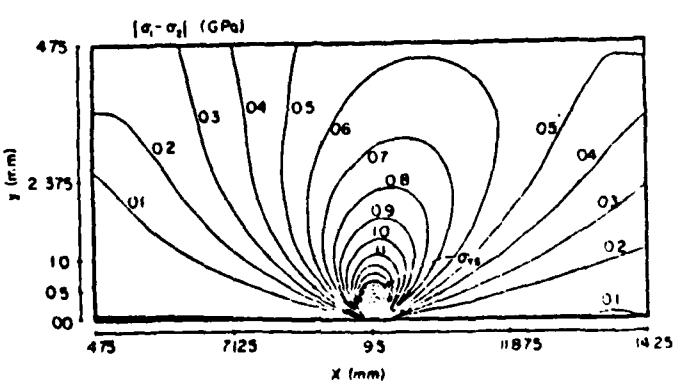

Figure 8

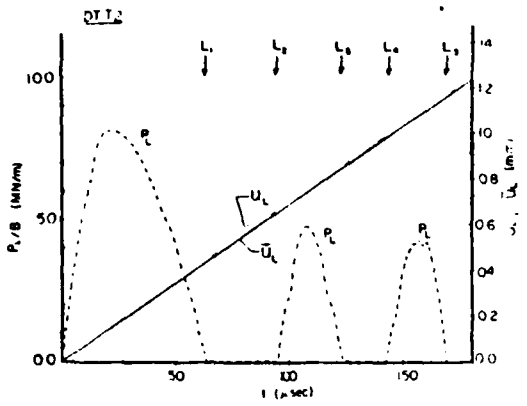

Figure 9

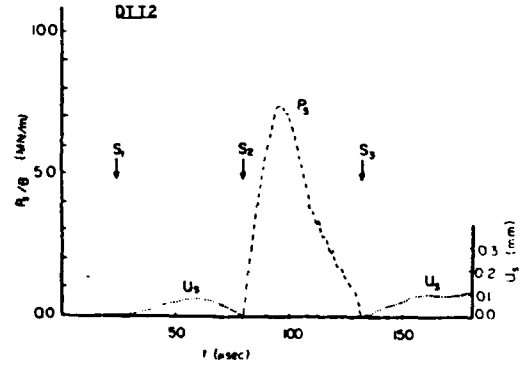

Figure 10

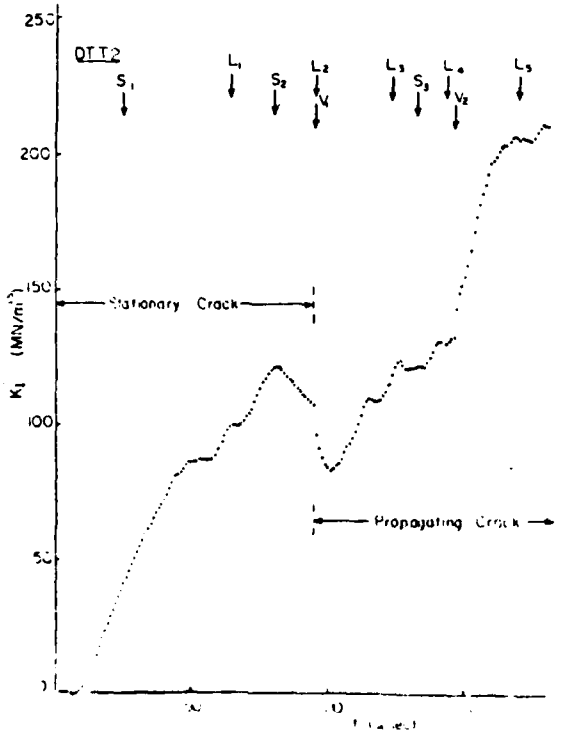

Figure 11

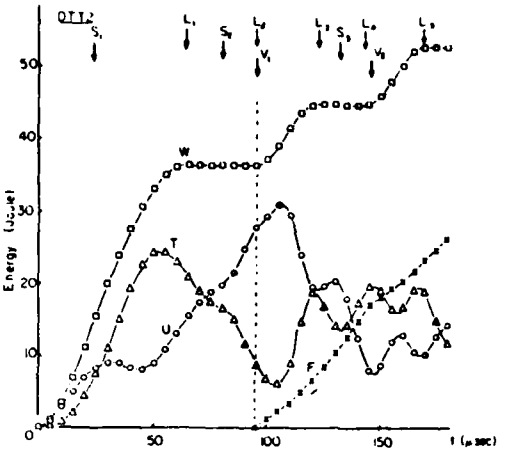

Figure 12

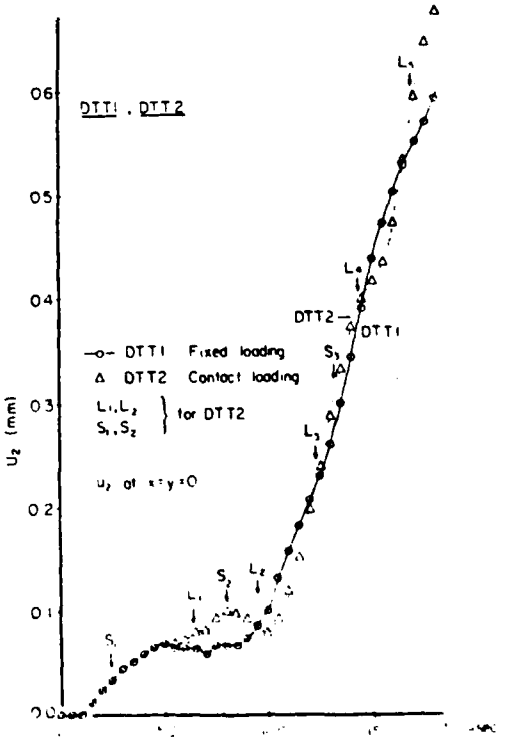

Figure 13

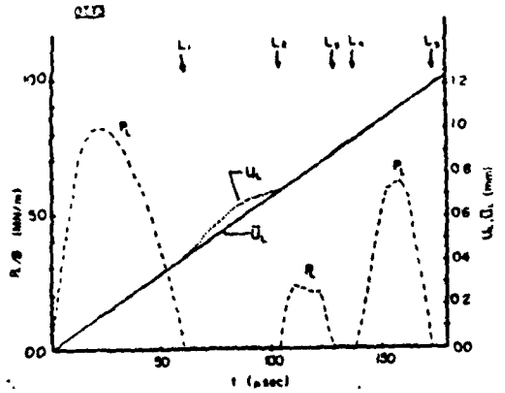

Figure 14

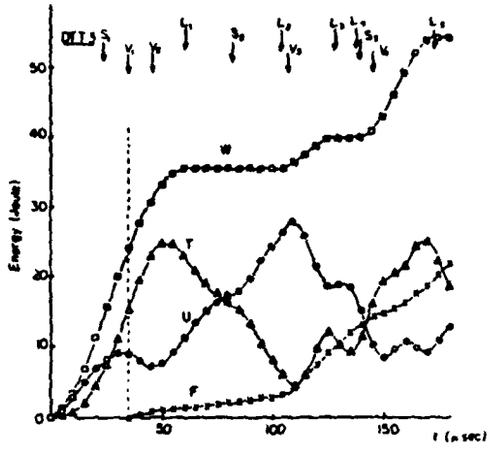

Figure 17

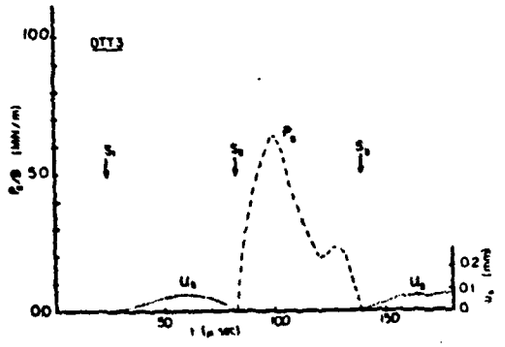

Figure 15

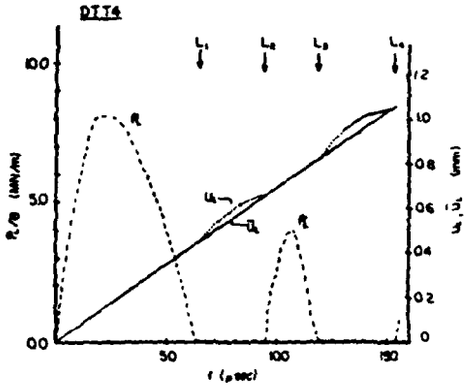

Figur 18

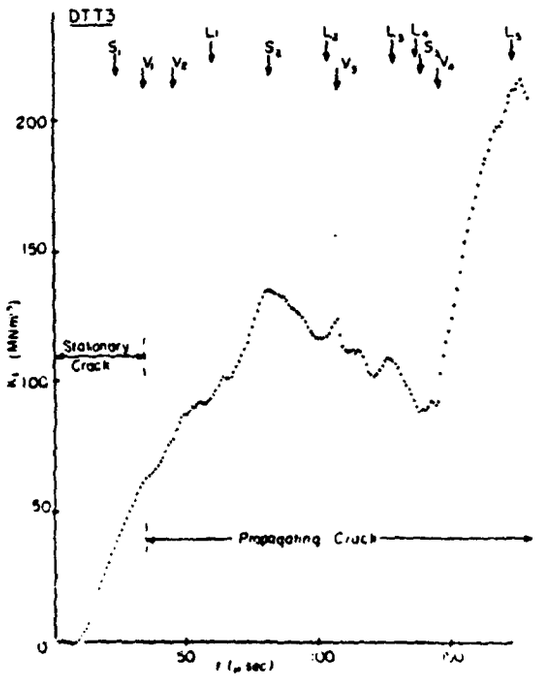

Figure 16

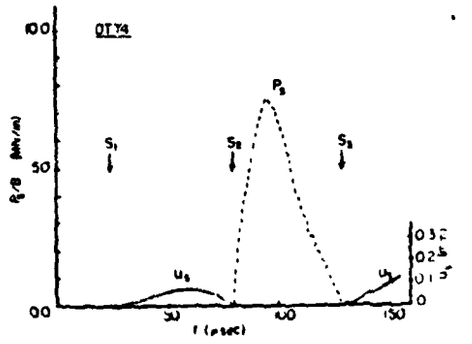

Figure 19

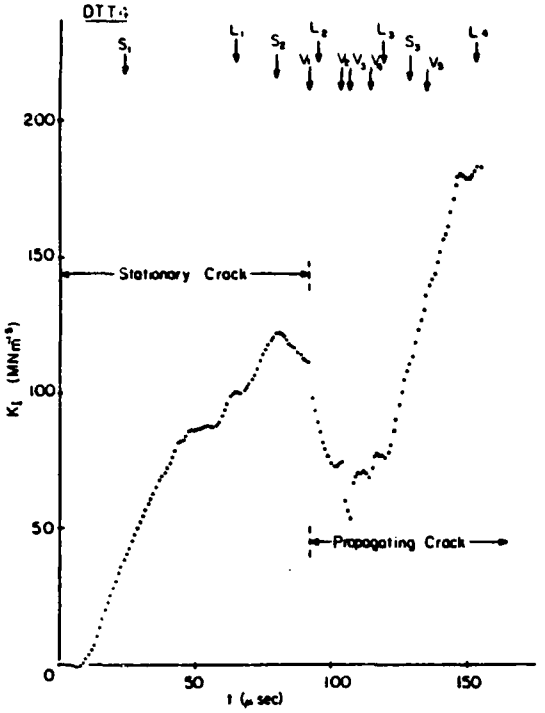

Figure 20

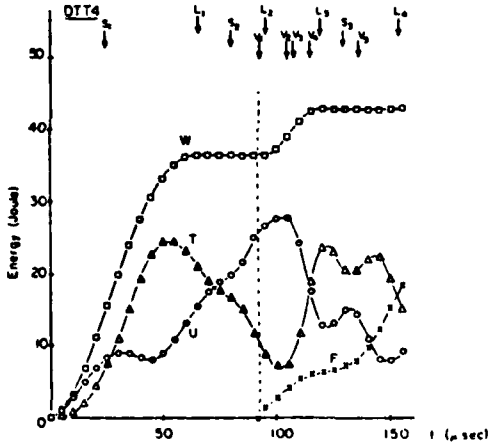

Figure 21

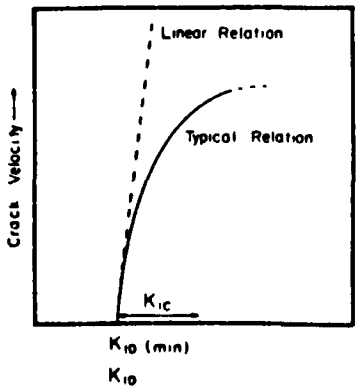

Figure 22

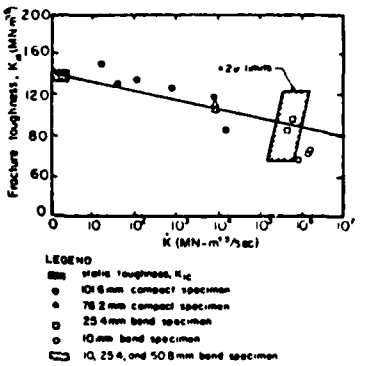

Figure 23

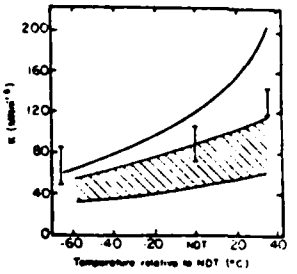

Figure 24

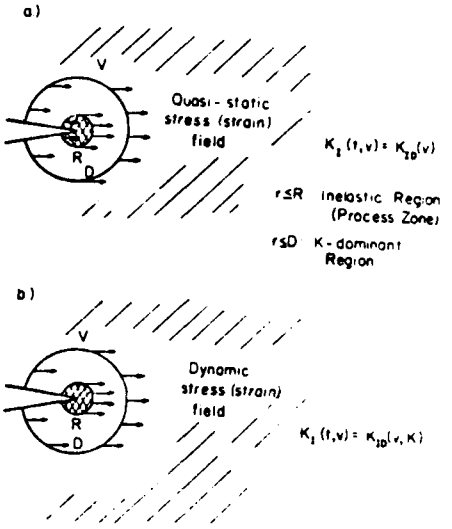

Figure 25

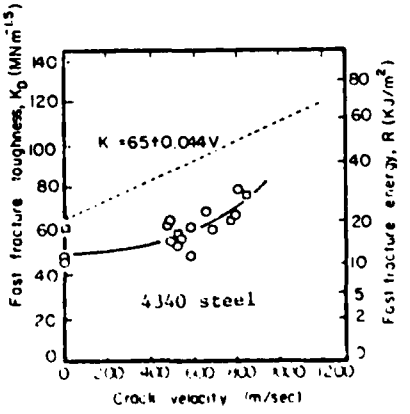

Figure 26

SECURITY CLASSIFICATION OF THIS PAGE (When Data Entered)

REPORT DOCUMENTATION PAGE	READ INSTRUCTIONS BEFORE COMPLETING FORM
1. REPORT NUMBER: 81-GIT-CACM-SNA-10 — 2. GOVT ACCESSION NO.: AD-A104216	3. RECIPIENT'S CATALOG NUMBER: 1
4. TITLE (and Subtitle): An Analysis of, and Some Observations on, Dynamic Fracture in an Impact Test Specimen	5. TYPE OF REPORT & PERIOD COVERED: Interim Report
	6. PERFORMING ORG. REPORT NUMBER: 81-GIT-CACM-SNA-10
7. AUTHOR(s): T. Nishioka, M. Perl, S.N. Atluri	8. CONTRACT OR GRANT NUMBER(s): N00014-78-C-0636
9. PERFORMING ORGANIZATION NAME AND ADDRESS: GIT - Center for the Advancement of Computational Mechanics, School of Civil Engineering, Atlanta, GA 30332	10. PROGRAM ELEMENT, PROJECT, TASK AREA & WORK UNIT NUMBERS: NR064-610
11. CONTROLLING OFFICE NAME AND ADDRESS: Office of Naval Research, Structural Mechanics Program, Dept. of Navy, Arlington VA 22217	12. REPORT DATE: July 1981
	13. NUMBER OF PAGES: 9
14. MONITORING AGENCY NAME & ADDRESS (if different from Controlling Office)	15. SECURITY CLASS. (of this report): Unclassified
	15a. DECLASSIFICATION DOWNGRADING SCHEDULE

16. DISTRIBUTION STATEMENT (of this Report)
Unlimited

17. DISTRIBUTION STATEMENT (of the abstract entered in Block 20, if different from Report)

18. SUPPLEMENTARY NOTES

19. KEY WORDS (Continue on reverse side if necessary and identify by block number)

20. ABSTRACT (Continue on reverse side if necessary and identify by block number)
Numerical simulations of crack-propagation histories in four cases of dynamic tear test experiments on 4340 steel are performed. The influence of the loss of contact of the specimen at various times with either the supports or the tup or both is critically examined. In each case, the variation of the dynamic K-factor, for the simulated crack-propagation history, is directly computed. The results are discussed in the light of current controversies surrounding the dynamic fracture toughness properties governing crack-propagation under impact loading. It is concluded that these controversies may not be fully warranted.

DD FORM 1 JAN 73 1473 EDITION OF 1 NOV 65 IS OBSOLETE

411865

SECURITY CLASSIFICATION OF THIS PAGE (When Data Entered)

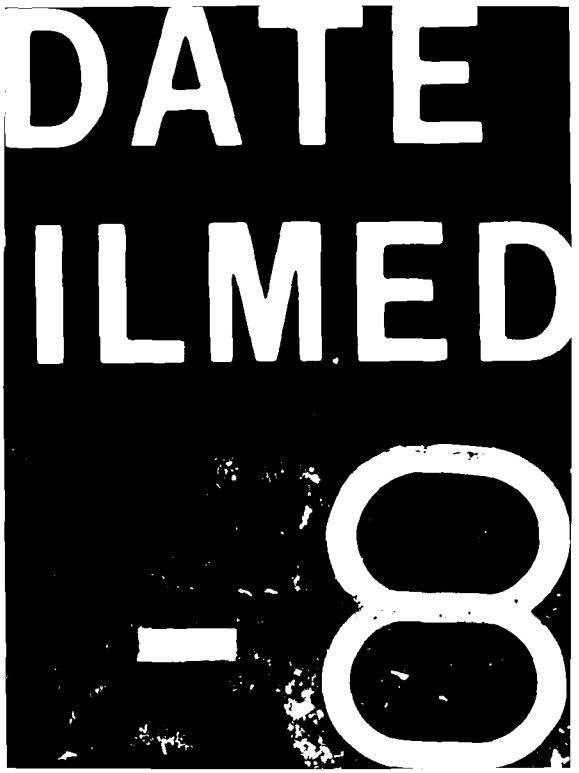
DATE
ILMED
-8